LBL-31748
Preprint

Lawrence Berkeley Laboratory
UNIVERSITY OF CALIFORNIA

Engineering Division

Submitted to X-Ray Spectrometry

High Precision Non-Destructive X-Ray Fluorescence Method Applicable to Establishing the Provenience of Obsidian Artifacts

R.D. Giauque, F. Asaro, F.H. Stross, and T.R. Hester

November 1991

U. C. Lawrence Berkeley Laboratory
Library, Berkeley

FOR REFERENCE

Not to be taken from this room

LBL-31748
Copy 1
Bldg. 50 Library.

Prepared for the U.S. Department of Energy under Contract Number DE-AC03-76SF00098

DISCLAIMER

This document was prepared as an account of work sponsored by the United States Government. While this document is believed to contain correct information, neither the United States Government nor any agency thereof, nor the Regents of the University of California, nor any of their employees, makes any warranty, express or implied, or assumes any legal responsibility for the accuracy, completeness, or usefulness of any information, apparatus, product, or process disclosed, or represents that its use would not infringe privately owned rights. Reference herein to any specific commercial product, process, or service by its trade name, trademark, manufacturer, or otherwise, does not necessarily constitute or imply its endorsement, recommendation, or favoring by the United States Government or any agency thereof, or the Regents of the University of California. The views and opinions of authors expressed herein do not necessarily state or reflect those of the United States Government or any agency thereof or the Regents of the University of California.

LBL-31748

High Precision Non-Destructive X-Ray Fluorescence Method Applicable to Establishing the Provenience of Obsidian Artifacts

Robert D. Giauque, Frank Asaro and Fred H. Stross
Lawrence Berkeley Laboratory
University of California, Berkeley CA, 94720

and

Thomas R. Hester
Texas Archeological Research Laboratory
University of Texas, Austin TX, 78712

November 1991

This work was supported by the Director, Office of Energy Research, Office of Biological and Environmental Research, Analytical Technology Division of the U.S. Department of Energy under Contract Number DE-AC03-76SF00098.

To be submitted to X-ray Spectrometry (February 1992)

High Precision Non-destructive X-ray Fluorescence Method Applicable to Establishing the Provenience of Obsidian Artifacts

Robert D. Giauque, Frank Asaro and Fred H. Stross
Lawrence Berkeley Laboratory
University of California, Berkeley, CA 94720
and
Thomas R. Hester
Texas Archeological Research Laboratory
University of Texas, Austin, TX 78712

Abstract

A high precision non-destructive x-ray fluorescence (XRF) method has been developed for the determination of both trace and major elements in obsidian archaeological artifacts. Other than brushing the artifact surface clean, no sample preparation is required. The method developed establishes XRF as an extremely valuable technique for the analysis of archaeological obsidian samples which cannot be sacrificed or altered because of their importance for historical studies. The method is applicable to both thick and thin samples which have wide variations in size and shapes. The method has been used to establish the provenience of a number of obsidian artifacts. The results ascertained for groups of samples from three proveniences are discussed in this paper.

The concentrations of thirteen trace (Ti, Mn, Zn, Ga, As, Rb, Sr, Y, Zr, Nb, Ba, Pb and Th) and three major elements (K, Ca and Fe) are determined from one x-ray spectrum

which is acquired during a 1000 sec counting interval. The concentrations of the six most precisely measured elements (Fe, Rb, Sr, Y, Zr and Ba) have yielded precisions which averaged 2.3%. The mean concentrations determined for five of these elements (excluding Y) differ on the average by only 2.0% from published values which were ascertained by neutron activation analysis (NAA) and XRF. The average standard deviations realized for the other ten elements determined was approximately 7%.

Introduction

Obsidian, a natural volcanic glass with extremely sharp edges when cleaved, was widely used in both prehistoric and historic times as a raw material for tools and weapons (1). Although pottery is the artifact material of choice in many archaeological studies, obsidian is especially important for those periods which predate pottery manufacture. Obsidian from a given source that is used for artifact production is usually chemically homogeneous, even for elements in minute concentrations. Obsidian from different sources have distinctly different element concentration patterns. Thus, in a manner similar to the use of fingerprints (2), the concentration pattern of the elements within an artifact, wherever it is found, can indicate the source (provenience) of the obsidian from which an artifact was made. These characteristics, together with its resistance to environmental deterioration, make obsidian a useful indicator of distribution networks and migratory activity of peoples of antiquity. Implicit in the use of "chemical fingerprinting" techniques is the need for a data bank of element concentrations for obsidian from all likely sources, analogous to the fingerprint files of the FBI.

The primary constituents in obsidian are silicon dioxide (75 – 80%), aluminum oxide (11 – 15%), and up to 5% of both sodium and potassium oxides. It is, however, the many trace and minor elements which have the large inter-source variations that make

chemical fingerprinting techniques successful (3). Even with trace elements, there is a significant probability that obsidian from two different sources will, within the errors of experimental measurements, have the same abundances for one or more given elements. This probability of agreement with chemical fingerprinting can be greatly reduced if the concentrations of many elements are determined, and the probability of agreement can be eliminated if such measurements are precise and accurate.

A number of multielement measurement techniques have been applied for analysis of obsidian artifacts. The earliest measurements were by emission spectroscopy (4) and X-ray fluorescence (2,5). Atomic absorption and flame photometry (6), as well as proton inelastic scattering (7) have also been applied. More recent studies have emphasized the application of NAA and more advanced XRF methods.

NAA analytical results (8), utilizing predominantly Na and Mn data, and to a lesser extent Sm, Sc, Rb, Fe and La data, were used in 1967 to demonstrate that obsidian artifacts, found in Ohio, Illinois, and Michigan, came from Obsidian Cliff in Yellowstone National Park. In 1968, Mesoamerican and Californian obsidians were studied. Data for 15 elements, determined by XRF, as well as Mn data measured by NAA (9) were used. In 1973, NAA measurements for 29 elements were carried out with sufficient precision and accuracy to demonstrate that obsidian from Borax Lake, California, was formed by the mixing of two lavas (10). NAA now provides a wide breadth of elements with good precision and accuracy (11-13) and has been unsurpassed in the ability of the technique to provide unambiguous assignments of provenience for obsidian artifacts. Additionally, NAA data can demonstrate when a chemical fingerprint is definitely new and to discern variability of element concentrations within a source. The costs of unsubsidized NAA measurements can be as high as hundreds of dollars per sample. The method also necessitates the destruction or mutilation of an artifact, which in many instances is not tolerable.

Although XRF measurements do not provide as large a breadth of precisely measured elements as does NAA, they are much less expensive and do not require a nuclear reactor. Measurements on samples prepared by destroying part of an artifact (destructive XRF) can produce precise data for a number of elements (14,15). With care this method has yielded elemental abundances of Rb, Sr, Zr and Ba with good precision, and of Y, Nb, Fe, Mn, Zn, La, Th and Ce with somewhat lower precision. Other elements accessible by this method have not been much used in connection with obsidian analysis.

The application of a non-destructive XRF method is critical for the assignment of the provenience of obsidian artifacts. Some artifacts cannot, or should not, be partially or wholly destroyed for the determinations. While some Mesoamerican sites, or other sites in close proximity to obsidian outcrops or obsidian trade routes, might yield hundreds or thousands of samples (thus permitting the use of a destructive analytical method), much obsidian source research involves: [1] unique artifacts, [2] areas and sites where obsidian rarely is found, and [3] the loan of obsidian artifacts from museums or private collectors.

First of all, with regard to unique artifacts, we can point to XRF studies of Paleoindian projectile points. These date between 8,000–11,000 BP and constitute irreplaceable indicators of early human activity. The occurrence of a Paleoindian obsidian artifact at a great distance from a source (e.g., an 11,000 year-old Clovis point from the Texas Gulf coast) (16) is important in studies of trade and group mobility. Non-destructive XRF is the most reasonable avenue for studies of this sort. Destructive analysis involving even a small segment of a unique artifact causes irreparable damage (17).

Secondly, obsidian source studies in regions where obsidian does not outcrop means that the archaeological samples are few and should not be destroyed for analytical

purposes. The Texas Obsidian Project (18) has devoted 20 years to the sourcing of approximately 150 artifacts from across that state. Destructive analysis would remove any possibility of such samples being studied at a later date via improved techniques.

Finally, many archaeological obsidian samples are in museum collections (or in collections within the purview of Federal agencies or foreign governments) and many have policies that do not allow destructive analysis. Other important artifacts are in the possession of private collectors, who will not loan the artifacts for analysis unless non-destructive methods are used.

XRF techniques are the most widely used for the analysis of obsidian artifacts in which the artifacts are not destroyed or mutilated (15,19-22). These techniques can be used by almost any laboratory which has XRF equipment and can be far less laborious than NAA determinations. Some of the reported results for non-destructive XRF have been strongly influenced by variations in the size or the shape of the artifacts. In order to minimize these effects, element concentration ratios often have been used (9,19,23) for elements which are close in atomic number, (e.g. Rb, Sr and Zr). Using this approach, many errors cancel out. Nevertheless, a significant fraction of the assignments of provenience are considered tentative until confirmed by high precision NAA (12).

There have been several studies in recent years concerned with the accuracy of non-destructive XRF measurements (20,24). A non-destructive method for the determination of eleven elements in obsidian artifacts has been reported (25,26). The method requires three separate excitation conditions for the determination of different groups of elements. Twenty six international geochemical standards were used to calibrate for most of the elements determined. Ratios of x-ray spectral line intensities to specific spectral background regions were applied. The method is mainly applicable if

the samples are close to infinite thickness for most of the radiation energies of interest. For thin samples, the ratios of x-ray spectral line intensities to the spectral background can vary with sample thickness. This is due to the fact that the ratio between spectral line intensity and spectral background does not become constant until the sample is of infinite thickness for the radiation energies of interest.

In the present work, we describe a non-destructive XRF method for the determination of sixteen elements in obsidian artifacts with a single measurement. The selection of the excitation radiation has been tailored to yield elemental concentration data for a maximum number of trace elements, with relatively high sensitivities being attained for most elements. The method is applicable to artifacts which vary greatly in size, shape, and thickness. The precisions and accuracies realized for the elements measured with the highest sensitivities rivals the results achieved by using high precision NAA.

Discussion of the Method

General technique for obtaining and characterizing the x-ray spectrum

X-rays provided by an x-ray tube or radioisotopes, either directly or indirectly with secondary targets, impinge upon a sample. A fraction of these photons, if of sufficient energy, produce vacancies in the inner shells of atoms within the sample, which in turn can emit characteristic x-rays that are measured by a semiconductor detector. In addition to these photoelectric interactions, a portion of the radiation striking the sample is scattered either coherently (no energy loss—Rayleigh scattering) or incoherently (with energy loss—Compton scattering). The energy loss by the Compton scattering process is a function of the energy of the primary radiation and the angle of scattering viewed by the detector system. For many element determinations, including the analysis of obsidian, the x-ray spectrum is composed primarily of scattered

excitation radiation and associated detector background produced via the detection of the intense scattered excitation radiation. Only a small fraction of the total radiation measured is characteristic x-rays from elements within the sample. It is these x-rays that are used for the determination of each of the individual elements measured. To obtain optimum sensitivity for elements which give rise to characteristic x-rays within a specific energy range, it is desirable to obtain maximum desired characteristic x-ray intensities, while minimizing the intensity of the spectral background at the energies of the radiations employed for analysis. Sensitivities realized vary proportionately with the signal to background and only by the square root of the characteristic x-ray spectral intensities. Thus, for example, if the signal to background could be improved by a factor of three by using one excitation radiation instead of another, one would need to count only one ninth as long to obtain equal counting statistics for the measurement, presuming that the total counting limitations of the detection system were the same in both cases.

High sensitivities with relatively high count rates can be realized using x-ray tubes indirectly with secondary targets. For these studies, we desired to obtain very high sensitivities for Rb, Sr, Y, Zr and Nb, as these elements are almost always present in obsidian artifacts at concentration levels which can be measured by XRF. The energies of the characteristic x-rays that are employed for analysis for these elements are in the 13 to 17 keV energy range. A minimum excitation radiation energy of 19 keV is required to excite Nb K x-rays from a sample. However, the bulk of the scattering of the excitation radiation realized is via the Compton scattering process. If the scattering is at an angle slightly greater than 90 degrees, the energy loss via single Compton scattering of a 20 keV radiation is approximately 1 keV. However, there is also second and third order Compton scattering that occurs and is detected from the obsidian samples. Consequently, to obtain optimum sensitivities for the above listed elements,

we have chosen a somewhat higher excitation energy than the minimum energy required for analysis.

Equipment and characteristics

The x-ray spectrometer system employed for these experiments is shown in Fig. 1. The x-ray system was designed and constructed by co-workers at our laboratory (27). It consists of a low power W-anode pulsed x-ray tube, automatic interchangeable secondary targets used to provide characteristic K x-ray secondary excitation radiation, a silicon guard-ring reject detector, and a 1024 channel pulse height analyzer. The total resolution of the system, FWHM, was 195 eV at 5.9 keV (Mn K-alpha x-ray energy) at 4000 cts/s using a 17 μs pulse peaking time.

For the measurements to be made on obsidian artifacts, a single secondary target, Ag, with a 0.025 cm Cu prefilter followed by a 0.015 cm Al filter was used to provide the excitation radiation. The x-ray tube was operated at 75 kV. The excitation radiation consisted primarily of Ag K-α (22.1 keV) and Ag K-β (25.0 keV) x-rays with a small amount of high energy Bremsstrahlung radiation with a maximum intensity at 39 keV. A Ag collimator, 0.64 cm long with an opening 0.32 cm in diameter, served to form a well defined near linear beam path for the radiation measured by the detector system. Thus, the collimator ensured that the detector efficiencies would be essentially constant for any given x-ray energy and not vary with positioning of the sample. Furthermore, the collimator closely defined the energy for the measured Compton scattered excitation radiation. The field of view seen by the detector system encompassed an area less than 1 cm^2. Spectral data were acquired by using a Nucleus PCA card in an IBM XT computer and were stored on disc. Computations were made by using a program that we established for these studies. The program required less than 40 K of memory.

Methodology and Calibration

Methodology

A six step approach is undertaken to calibrate the spectrometer system. The following lists a brief description of each of the steps which will be described in detail later in this section.

The first step entails calculation of values for the incoherent scattering coefficients and total mass absorption coefficients at specific x-ray energies for the range of obsidian artifact compositions encountered. Data from the literature are used for these calculations. The results of the calculations will clearly demonstrate that the incoherent scattering coefficients encountered are essentially constant for the excitation radiations employed for our experiments. Furthermore, the calculations will illustrate that varying composition of three major elements that are measured, K, Ca and Fe, are essentially the sole consideration for variations in the total mass absorption coefficients for the energy range of interest for obsidian artifacts.

For the second step, the use of thin sections of extremely high purity quartz of known mass thickness are employed to calibrate the spectrometer system for the determination of the sample mass thickness and matrix absorption effects. The matrix absorption effects include the attenuation of the excitation and the Compton scattered radiations. This step is a crucial part of the method. In this step, the relative intensities of two Compton scattered excitation radiations (Ag K-α and Ag K-β) are applied to ascertain the sample mass thickness and the mass absorption coefficients.

The third step involves the use of single element thin film deposits to establish the spectrum channels to be employed for the specific characteristic x-ray lines to be

utilized for analysis. The spectra for these deposits are also used to establish the individual spectral peak overlaps (e.g. the K-β x-ray line from one element with the K-α x-ray line of another element). For a few elements which often can have relatively intense characteristic spectral lines (Fe, Rb, Sr, Y, Zr and Nb) when carrying out the analysis of the obsidian artifacts, pure element compounds are blended at low concentrations with high purity sand to obtain the peak shapes at x-ray energies just below that of the characteristic spectral line used for analysis.

The spectra obtained for the thin sections of extremely high purity quartz are used for the fourth step. Relationships are established between three scattered excitation radiation intensities and the spectral scattered radiation background at the energy regions to be employed for the individual element determinations.

For the fifth step, two multielement thin film standards are used to ascertain the relative response of the spectrometer system for the excitation and detection of characteristic x-rays from the range of elements of interest. The relative excitation and detection values apply for very thin samples with no matrix absorption effects.

The sixth step entails the use of a source obsidian which has been very well characterized by NAA to standardize the spectrometer system for the determination of five elements (K, Mn, Fe, Th and Ba). For the other eleven elements, actual standardization is interpolated using data from the two multielement thin film standards used in step 5.

Calculation of incoherent scattering coefficients and total mass absorption coefficient values for obsidian artifacts

Andermann and Kemp (28) initially demonstrated that the intensity of scattered excitation radiation could be employed as an internal standard for some XRF determinations. Reynolds (29-30) and Feather and Willis (31) initially used the intensity of Compton scattered excitation radiation to compensate for matrix effects for the determination of trace elements in geochemical samples. The approach exploits the fact that, if the sample is infinitely thick for the radiation energies of interest, the intensity of the Compton scattered excitation radiation varies linearly with the reciprocal of the mass absorption coefficient of the sample.

The XRF method described in this paper is applicable to both thick and thin obsidian samples. The method makes use of the intensities of two Compton radiations simultaneously scattered at different x-ray energies. Both composition and thickness of the sample affect the relative intensities of measured x-ray spectral lines as well as the intensities of the scattered excitation radiations. Initially we will show that with due consideration, the degree to which obsidian artifacts of varying composition attenuate x-rays can be calculated. This information is coupled with the determination of the sample mass thickness using an iterative procedure, and matrix absorption effects are ascertained for all x-ray energies of interest.

For the purpose of this paper, the obsidian is treated as being composed of two major element component groups. One component group consists of low atomic number element oxides, Na_2O, Al_2O_3 and SiO_2. The concentrations of the low atomic number group are not determined by the XRF method to be described. The second component group consists of somewhat higher atomic number element oxides, K_2O, CaO, and Fe_2O_3. The concentrations of these higher Z elements are measured by our XRF

method. These are the elements, as will be shown later, that are solely responsible for the differences in the mass absorption coefficients for obsidian artifacts from different sources. Listed in Table 1 are the typical major element oxide concentration ranges for obsidian artifacts.

For our method, the intensities of two separate Compton scattered excitation radiations in the energy range of 20 to 24 keV are simultaneously employed to ascertain information regarding sample mass thickness and composition. For any given energy and fixed angle of scattering, the relative degree to which samples of varying composition Compton scatter radiation can be calculated using equation 1:

$$\sigma_{Incoh.} = \sum_{i=1}^{n} \sigma_i W_i \qquad (1)$$

where σ_i and W_i are the incoherent scattering coefficient (cm^2/g) and the weight fraction of element i, respectively. In effect, the total incoherent scattering coefficient of a sample is the sum of the products of the weight fraction of each element and the incoherent scattering coefficient of the element for the incoming radiation to be incoherently scattered.

Using data from x-ray cross section tables published by McMaster *et al.* (32), we have calculated the incoherent scattering coefficients at two x-ray energies, 20 and 24 keV, for two very different hypothetical obsidian samples. One sample contains a minimum weight fraction of the low Z elements shown in Table 1, and the second contains a maximum weight fraction for the low Z elements. These hypothetical samples represent the extreme range likely to be encountered for obsidian artifacts. The results of the calculations are listed in Table 2.

For these two hypothetical obsidian samples, the incoherent scattering coefficients at each of the two energies vary by a maximum of 0.5%. Furthermore, for each of the two samples, the ratios of the incoherent scattering coefficients for the two energies, 20 and 24 keV, deviate by only 0.1%. Thus, for the range of real world obsidian samples, the ratios of the incoherent scattering coefficients can be considered to be essentially constant for the energy range listed.

The absorption correction for a homogeneous sample integrated over a mass thickness, m(g/cm^2), may be expressed:

$$Ab_{corr} = \mu m / (1 - e^{-\mu m}) \qquad (2)$$

The mass absorption coefficient term, μ(cm^2/g), is determined by summing the contribution of each element and is correctly expressed:

$$\mu = \sum_{i=1}^{n} (\mu_1^e \csc \Psi_1 + \mu_2^f \csc \Psi_2) W_i \qquad (3)$$

where μ_1^e and μ_2^f are the total mass absorption coefficients of element i for the excitation and the emitted characteristic radiations, respectively; and Ψ_1 and Ψ_2 are the angles formed by the excitation and the detected characteristic radiations with the surface of the sample.

Using data from the x-ray cross section tables listed above, we have calculated the total mass absorption coefficients at six x-ray energies for the range of compositions likely to be encountered for obsidian artifacts. One sample is assumed to contain a minimum weight fraction of the low Z elements and would give rise to maximum mass absorption coefficient values. Conversely, the other sample is assumed to contain a

maximum weight fraction of the low Z elements and would give rise to minimum mass absorption coefficient values. The values calculated are shown in Table 3. Also listed in Table 3 are the total mass absorption coefficients that would be realized for a matrix composed of the low Z fraction of the elements only. These latter values were calculated by dividing the contribution of the low Z component to the total mass absorption coefficient by the total weight fraction of the low Z component. For the six x-ray energies listed, an average deviation of only 0.3% is calculated for the total mass absorption coefficients for the two extremes in composition for the low Z fraction that can potentially be encountered. Thus, the total mass absorption coefficient for the low Z component of the matrix can be considered to be essentially constant, and only the weight fraction of this component need be ascertained. Deviations in the weight fractions of the higher atomic number element oxides (K_2O, CaO and Fe_2O_3) are solely responsible for the deviations in the total mass absorption coefficients for each of the listed energies in Table 3. The weight fractions for each of the three higher atomic number elements are determined by using our approach described in this paper, and mass absorption coefficient values are calculated for all x-ray energies of interest.

Calibration of the spectrometer system for the determination of the sample mass thickness

As mentioned earlier, our method uses the relative intensities of the Compton scattered Ag K-α (20.7 keV) and the Ag K-β (23.15 keV) x-rays as a measure of the sample mass thickness. This is possible, since as the sample mass thickness increases, absorption effects increase more rapidly for the lower energy incoming and Compton scattered Ag K-α radiation than they do for the corresponding Ag K-β radiation. Once infinite thickness is realized for the higher energy Ag K-β x-rays, the ratios of the relative intensities of the two Compton scattered radiations should become constant. To illustrate this, we used thin sections (0.080 cm thick or 0.180

g/cm^2) of very high purity quartz. The relative intensities of the Compton scattered Ag K x-rays for various numbers of stacked thin sections of quartz were measured. Figure 2 show a plot of the ratios for the two Compton scattered radiation intensities (Ag K-β/Ag K-α).

Using the zero intercept ratio value (no x-ray absorption), mass thicknesses of quartz were calculated for each of the measurements using equations 2 and 3. The angles formed by the excitation and the scattered radiations with the sample surface were both assumed to be 65 degrees. Listed in Table 4 are the true and the calculated mass thicknesses which differ on the average by only 0.8%. Thus, the mass thickness of obsidian samples can be determined from the relative intensities of the two Compton scattered Ag K radiations, if at the same time, appropriate calculations are made regarding the concentrations of K_2O, CaO, and Fe_2O_3. The weight fractions of these element oxides can be ascertained experimentally, as described later, in an iteration procedure which makes use of the measured x-ray spectral line intensities for K, Ca, and Fe. Once the concentrations of the major element components are established, along with the mass thickness of the sample, matrix absorption effects are calculated for all of the other x-ray energies of interest.

X-ray spectral line overlaps

Relationships for most x-ray spectral line overlaps were ascertained from thin deposits of each element on teflon filters. X-ray matrix absorption effect adjustments are calculated during the analysis for some of the x-ray spectral line overlaps (e.g. Rb K-β with Y K-α). For the elements Fe, Rb, Sr, Y, Zr and Nb, element compounds were mixed with high purity sand and x-ray spectral line overlaps were established for the energy region within 2 keV below the energy of the K-α spectral line. The reason for using this procedure was that the thin deposits do not yield accurate x-ray spectral

peak overlaps for this energy region. A small fraction of the relatively intense K-α x-ray spectral line is scattered within the sample, and thus produces a slightly higher tailing x-ray spectral line overlap in the above mentioned energy region.

Spectral background due to scattered excitation radiation

The spectra acquired from the stacked thin sections of very high purity quartz were used to established the spectrum background equations for each of the x-ray spectral lines to be employed in our determinations. We used fixed number of channels for each x-ray spectral line. Typically, the fixed channels used encompassed approximately 90% of the counts for the specific x-ray spectral line. Equations which related the intensity of the scattered excitation radiation spectral background, for each of the x-ray spectral lines employed, to the intensities of three scattered excitation radiations, Compton scattered Ag K-α, Compton scattered Ag K-β, and scattered high energy Bremsstrahlung, were established.

Calibration of the relative response of the spectrometer system for the excitation and the detection of characteristic spectral x-rays

Two multielement thin film standards on teflon filters were used to calibrate the relative response of the spectrometer system for the excitation and detection of characteristic x-rays from the range of elements of interest. The first thin standard contained Ca, Ti, Mn, Cu and Ge and the second contained V, Fe, Ni, Zn Rb, Sr and Pb. The method used to prepare the standards and determine the precise mass loadings of the individual elements has been described (33). The relative response of the spectrometer system for the excitation and detection of characteristic K-α spectral lines from the elements is illustrated in Fig. 3. The x-axis, K_{ab}, is the K x-ray critical absorption edge energy for the elements listed.

Standardization of the spectrometer system using obsidian from a source which has been well-characterized by NAA

Standardization of the system was achieved by using pieces of obsidian from a very well characterized source, El Chayal, Guatemala (11). The NAA results for K, Mn, Fe, Th and Ba served as reference values. The relative response for the remaining eleven elements determined were ascertained from the two multielement thin standards.

For any given sample mass thickness, x-ray spectral line intensities can vary with sample size, if the field of view seen by the detection system is not completely covered. Consequently, the intensity of the Compton scattered Ag K-α radiation, corrected for matrix absorption effects, is used to serve as an internal standard, for all of the elements determined except Ba, to compensate for variations in sample size. The intensity of the high energy Bremsstrahlung radiation scattered in the energy range of 39.0 to 42.5 keV, corrected for matrix absorption effects, served as the internal standard for the determination of Ba.

As mentioned above in the section on Equipment and Characteristics, a pulsed x-ray tube was employed for our determinations. Since the pulsed x-ray tube was not linked with the computer system used to acquire spectra, it was not possible to obtain the spectra using a fixed number of x-ray beam dumps. Thus, fixed time counting intervals of 1000 sec were employed. Consequently, depending upon the sample size and thickness, variable amounts of excitation radiation are utilized for analysis. A plastic cell with a 5 μm thick polypropylene film window was used to contain the sample. A small fraction of the excitation radiation was scattered from the air and the polypropylene film window. Additionally, the air between the sample and the detector gave rise to Ar K x-rays in the x-ray spectra. To account for the very small amount of system background (due to the air and the thin polypropylene film window), a thin strip

of 10 μm Mo foil was positioned in the spectrometer in front of the sample holder and at the periphery of the beam path. The intensity of the x-rays from the Mo foil served as an x-ray beam monitor. The small amount of system background was ascertained by acquiring a spectrum for the empty cell with the Mo foil monitor only.

A flowchart showing the steps undertaken for the determination of thirteen trace and three major elements in obsidian artifacts is illustrated in Fig. 4.

Results

Two experiments were selected to study the precision and the accuracy of the method for source material and artifacts, and in the process, determine if untreated surfaces of artifacts presented any measurement or interpretation problems.

In the first experiment, four pieces of freshly-cleaved obsidian, which were considerably different in size and shape, from the El Chayal source in Guatemala were measured as a check on the precision of the method. It was not possible to check the accuracy of the method for K, Mn, Fe, Ba and Th in this experiment, because El Chayal obsidian was used to standardize the spectrometer system for these elements. A photograph of the four pieces of obsidian is shown in Fig. 5. Prior to analysis, the surface which was the flattest was brushed with a stiff bristle brush to remove possible surface contaminants. The flattest surface of the obsidian was placed facing the detector. For each piece, values were calculated for: 1. sample mass thickness, 2. absorption corrections for each X-ray energy of interest, and 3. individual element concentrations using equation 4:

$$C_i = I_i \times Ab_i \times K_i \times C / (I_{Incoh.} \times Ab_{Incoh.}) \qquad (4)$$

where I_i and $I_{Incoh.}$ are the intensities of the characteristic spectral line from element i and the Compton scattered Ag K-α radiations, respectively; Ab_i and $Ab_{Incoh.}$, are the absorption corrections calculated for the respective radiations; K_i is the relative excitation-detection efficiency ascertained for element i from the multielement deposits on teflon filters or from one of the five elements of the El Chayal source used to standardize the spectrometer system; and C is an overall system calibration constant. The system calibration constant was ascertained for a single element, Fe, for which the concentration had been previously established by NAA. The element abundances determined for the four pieces of El Chayal source obsidian are listed in Table 5. Thus, for a broad range of sample sizes and shapes, results with high precision were realized. The mean precision obtained for all sixteen elements was 4.4%. Figure 6 is a plot of the x-ray spectrum acquired for the large piece of obsidian listed in Table 5.

In the second experiment, measurements were made on 12 obsidian artifacts collected in Texas as part of an archaeological study program (the Texas Obsidian Project) at the University of Texas at Austin. The artifacts ranged in thickness from 1 to 5 mm, and many were smaller than the field of view observed by the detector. The only treatment applied to the artifacts was a brushing with stiff bristles prior to the measurements. The results of the analyses, which are shown in Tables 6 and 7, indicate that the 12 artifacts should be equally divided into two chemical groups, one originating from an obsidian deposit near Malad, Idaho and the other from the Cerro Toledo Rhyolite in the Valles Caldera in New Mexico. The range of the mass thicknesses determined for the artifacts from the two sources listed in Tables 6 and 7 were 0.34 – 1.63 g/cm^2, and 0.29 – 0.85 g/cm^2, respectively. The average precision for the six most precisely measured elements in Tables 5 – 7 is 2.3%, comparable to the average of 1.9% for the sixteen most precisely measured elements by NAA in two large groups of artifacts from Belize (11).

For Fe and higher Z elements, the precisions of measurement for the artifacts, whose surfaces were aged, were comparable to those of the El Chayal source obsidian, whose surfaces were freshly-cleaved. The lower Z elements had poor precision in the artifact groups. This was due to lower sensitivities realized for the determination of these elements as well as more severe peak overlap problems. Additionally, surface effects become a consideration at lower x-ray energies.

Comparison of our data with prior NAA measurements for K, Mn, Fe, and Ba show differences averaging about 3.5%. Comparison with prior XRF measurements for Rb, Sr (>>1 ug/g), and Zr show average differences of 3.7%. If we consider only those elements which: 1) give rise to characteristic x-rays of energy greater than 6.0 keV, 2) do not have any substantial unresolved peak overlap problems, and 3) were measured with a precision better than 5%, then the average difference between the current and earlier work is 2.0% (Malad references – Rb, Sr and Ba measured by XRF and Fe by NAA; Cerro Toledo Rhyolite references – Rb and Zr measured by XRF and Fe by NAA).

There are discrepancies, however, for Th measured by NAA and Ti, Sr at the μg/g level, Y, and Nb measured in other studies by XRF. The former discrepancy probably reflects a problem in the subtraction of background under the Th peak, but the origin of the discrepancies with the XRF data has yet to be determined.

Conclusions

In summary, a non-destructive XRF method applicable to the analysis of obsidian artifacts has been developed. The method can be used for both thick and thin samples of varying shapes. Most important, the method permits the integrity of historical obsidian artifacts to be preserved. Yet, the method yields relatively high precision

elemental concentration data for thirteen trace and three major elements. The element concentration information obtained can be used to assign the provenience of most obsidian artifacts.

In a separate paper, we described in detail that it is more important to obtain high precision results for a few elements than it is to obtain poor precision for many elements for the purpose of assigning the provenience of an obsidian artifact (34). In the paper, we show that the XRF method should often permit the provenience of an artifact from known sources to be established with a certainty better than 99.99%. The XRF method is not as useful as NAA in distinguishing elemental concentration variations within a source. However, with further refinements to the method for the determination of Y, Mn, and low level concentrations of Sr and Ba, the method could be as useful as NAA for the determination of the geochemical origin of artifacts from a source with a variable composition. The ability of the method to non-destructively ascertain quickly, reliably, and inexpensively the provenience (from any known sources) of valuable artifacts of any size or shape is probably unmatched at the present time.

Acknowledgment

This work was supported by the Director, Office of Energy Research, Office of Biological and Environmental Research, Analytical Technology Division, U.S. Department of Energy under Contract No. DE-AC03-76SF00098.

References

1. L. Aveleyra Arroyo de Anda and M. Maldonado-Koerdell, *Revista Mexicana de Estudios Antropologicos* **13**(1), 3 (1952).
2. J.R. Weaver and F.H. Stross, *Contrib. Univ. Calif. Archaeol. Res. Facility* **1**, 89 (1965).
3. R.N. Jack, *Advances in Obsidian Glass Studies—Archaeological and Geochemical Perspectives*, R.E. Taylor, Ed., Noyes Press, Park Ridge, New Jersey, 183 (1976).
4. J.R. Cann and C. Renfrew, *Proc. Prehistoric Soc.* **30**, 111 (1964).
5. G.A. Parker and T.T. Tieh, *Nature* **211**, No.5046, 289 (1966).
6. G.C. Armitage, R.D. Reeves and P.S. Bellwood, *New Zealand Journal of Science* **15**, 408 (1972).
7. G.E. Coote, N.E. Whitehead and G.J. McCallum, *Journal of Radioanalytical Chemistry* **12**, 41 (1972).
8. A.A. Gordus, W.G. Fink, M.E. Hill, J.C. Purdy and T. Wilcox, *Archaeometry* **10**, 87 (1967).
9. F.H. Stross, J.R, Weaver, G. Wyld, R.H. Heizer and J. Graham, *Contrib. Univ. Calif. Archaeol. Res. Facility* **5**, 59 (1968).
10. H.R. Bowman, F. Asaro and I. Perlman, *J. Geology* **81**, 312 (1973).
11. F. Asaro, H.V. Michel, R. Sidrys and F. Stross, *Am. Antiquity* **43**, 436 (1978).
12. F.H. Stross, P. Sheets, F. Asaro and H.V. Michel, *Am. Antiquity* **48**, 323 (1983).
13. R.H. Cobean, J.R. Vogt, M.D. Glascock, T.L. Stocker, submitted to *Am. Antiquity*, N.D.
14. F.W. Nelson, *Contrib. Univ. Calif. Archaeol. Res. Facility* **45**, 27 (1984).
15. J.H. Hampel, *Contrib. Univ. Calif. Archaeol. Res. Facility* **45**, 21 (1984).
16. T.R. Hester, *Paleoindian Artifacts from Texas: A Review, Current Research in the Pleistocene* **5**, 27 (1988).

17. T.R. Hester, F. Asaro, F. Stross, H. Michel, A. Kerr and P. Headrick, *An Overview of the Results of the Texas Obsidian Project, La Tierra* **18**, 4, Jour. S. Texas Archaeol. Assoc., San Antonio (1991).

18. T.R. Hester, G. Evans, F. Asaro, F. Stross, T. Campbell and H. Michel, *Bull. Texas Archaeol. Soc.* **56**, 143 (1985).

19. P.M. Rice, H.V. Michel, F. Asaro and F. Stross, *Am. Antiquity* **50** (3), 591 (1985).

20. R.E. Hughes, *Bull. So. Calif. Acad. Sci.* **85** (1), 35 (1986).

21. R.E. Hughes, *Texas J. Sci.* **40**, 297 (1988).

22. M.S. Shackley, *Am. Antiquity* **53** (4), 752 (1988).

23. R.N. Jack and I.S.E. Carmichael, *Calif. Div. Mines and Geology* **SR 100**, 17 (1968).

24. P.D. Bouey, in press, *Proc. Materials Res. Symposium* (1990).

25. R.E. Hughes, *Geoarchaeology* **3** (4), 253 (1988).

26. R.E. Hughes and W.B. Lees, *Transactions of the Kansas Academy of Science* **94** (1-2), 38 (1991).

27. J.M. Jaklevic, F.S. Goulding, B.V. Jarrett and J.M. Meng, in *Analytical Methods Applied to Air Pollution Research*, R.K. Stevens, W.F. Herget, Ed., Ann Arbor Science, Ann Arbor, Michigan (1974).

28. G. Andermann and J.W. Kemp, *Anal. Chem.* **30**, 1306 (1958).

29. R.C. Reynolds, Jr., *Am. Mineral* **48**, 1133 (1963).

30. R.C. Reynolds, Jr., *Am. Mineral* **52**, 1493 (1967).

31. C.E. Feather and J.P. Willis, *X-ray Spectrom.* **5**, 41 (1976).

32. W.H. McMaster, N. Kerr Del Grande, J.H. Mallett and J.H. Hubbell, *Compilation of X-ray Cross Sections*, University of California, Lawrence Livermore Laboratory Report, UCRL-50174, Section II, Revision 1 (1969).

33. R.D. Giauque, J.M. Jaklevic and A.C. Thompson, *Anal. Chem.* **58**, 940, (1986).

34. F. Asaro, R.D. Giauque and F.H. Stross, submitted to *Am. Antiquity* (1992).

35. T.R. Hester, F. Asaro, H. Michel, F. Stross and F.W. Nelson, *Prehist. Sites Choke Canyon Reservoir, S. Texas: Results of Choke Canyon Series 10*, Center for Archaeol. Res., Univ. Texas at San Antonio, 512 (1985).

36. T.R. Hester, F. Asaro, H. Michel, F. Stross, A.C. Kerr and R.D. Giauque, *Studies in Archaeology* **8**, T.A.R.L., Univ. Texas at Austin (1991).

Table 1.

Typical Major Element Oxide Concentration Ranges for Obsidian Artifacts

Major Element Oxides	Wt. %
Not to be determined by XRF	
Na_2O	4 – 5
Al_2O_3	11 – 15
SiO_2	75 – 80
To be determined by XRF	
K_2O	4 – 5
CaO	0 – 1
Fe_2O_3	0.3 – 3

Table 2.

Calculated Incoherent Scattering Coefficients

Energy			Incoherent Scattering Coeff. (cm^2/g) of Mixture 20 keV	24 keV
	Element Oxide	Wt %		
Minimum Low Z Wt. Fraction				
	Na_2O	4		
	Al_2O_3	11		
	SiO_2	76		
	K_2O	5		
	CaO	1		
	Fe_2O_3	3		
			0.1455	0.1506
Maximum Low Z Wt. Fraction				
	Na_2O	5		
	Al_2O_3	15		
	SiO_2	75.7		
	K_2O	4		
	CaO	0		
	Fe_2O_3	0.3		
			0.1462	0.1512

Table 3.

Calculated Total Mass Absorption Coefficients

	Total Mass Absorption Coeff. (cm^2/g) of Mixture					
Energy (keV)	4	8	12	16	20	24
Minimum Low Z Wt. Fraction (Table 2)	287.1	47.2	14.62	6.32	3.32	1.99
$Na_2O+Al_2O_3+SiO_2$ component/0.91	264.7	36.4	10.91	4.65	2.44	1.47
Maximum Low Z Wt. Fraction (Table 2)	284.4	40.4	12.26	5.24	2.75	1.65
$Na_2O+Al_2O_3+SiO_2$ component/0.96	264.1	36.2	10.88	4.64	2.43	1.47

Table 4.

Thickness of High-purity Quartz Thin Sections

No. of Quartz Thin Sections	True Mass Thickness (g/cm^2)	Calculated Mass Thickness (g/cm^2)
1	0.180	0.179
2	0.360	0.361
3	0.540	0.548
4	0.720	0.715
5	0.900	0.903
6	1.080	1.094

Table 5.

Element Concentrations Determined for Four Source Samples of Varying Shapes and Sizes from El Chayal, Guatemala
(μg/g ± 1σ unless otherwise indicated)

Sample Description	Large	Medium Long	Medium Short	Small						
Calculated Mass Thick. (g/cm^2)	2.00	0.92	0.35	0.45						
Element	Determined Concentrations				Mean Value			NAA Values Used for Calibration*		
K%	3.54	3.55	3.72	3.43	3.56	±	0.12	3.45	±	0.26
Ca%	0.66	0.75	0.76	0.75	0.73	±	0.05			
Ti	817	766	815	859	814	±	38			
Mn	635	651	686	630	651	±	25	649	±	13
Fe%	0.589	0.603	0.641	0.595	0.607	±	0.023	0.627	±	0.027
Zn	42	47	44	43	44	±	2			
Ga	21	20	21	19	20	±	1			
As	9.6	10.9	10.6	11.0	10.5	±	0.7			
Rb	146	150	150	144	147	±	3			
Sr	151	155	152	147	151	±	3			
Y	17.1	16.4	16.6	16.5	16.7	±	0.3			
Zr	107	107	105	103	106	±	2			
Nb	15.5	15.9	17.2	15.8	16.1	±	0.7			
Ba	948	889	898	915	913	±	26	915	±	35
Pb	18.7	19.0	17.1	17.6	18.1	±	0.9			
Th	10.5	11.6	11.7	12.2	11.5	±	0.7	10.4	±	0.1

* After calibration was achieved, the x-ray peak overlap corrections were changed slightly before the measurements in Table 5 were made. Consequently, the mean values determined above are slightly different from the input NAA calibration values used (11).

Table 6.

Element Concentrations of Six Obsidian Artifacts Attributed to Malad, Idaho Source
(μg/g ± 1σ unless otherwise indicated)

Element	Mean Value Determined			NAA Ref. 35			XRF Ref. 14		
K%	4.10	±	0.36	4.05	±	0.27			
Ca%	0.57	±	0.06						
Ti	547	±	44				400	±	60
Mn	221	±	18	206	±	4	248	±	8
Fe%	0.69	±	0.02	0.71	±	0.02	0.68	±	0.01
Zn	38	±	2						
Ga	23	±	1						
Rb	127	±	1	134	±	5	127	±	3
Sr	74	±	1				77	±	3
Y	27	±	1				9	±	8
Zr	87	±	1				86	±	6
Nb	19	±	2				7	±	4
Ba	1560	±	40	1500	±	16	1628	±	12
Pb	31	±	1						
Th	19	±	1	22.1	±	0.2			

Table 7.

Element Concentrations of Six Obsidian Artifacts
Attributed to Cerro Toledo Rhyolite, New Mexico Source
(μg/g ± 1σ unless otherwise indicated)

Element	Mean Value Determined			NAA Ref. 36			XRF Ref. 14		
K%	3.90	±	0.23	3.86	±	0.22			
Ca%	0.11	±	0.02						
Ti	292	±	47				432	±	6
Mn	550	±	32	564	±	11	636	±	8
Fe%	0.78	±	0.02	0.787	±	0.014	0.84	±	0.01
Zn	103	±	6						
Ga	39	±	2						
Rb	208	±	4	210	±	14	198	±	2
Sr	0.8	±	0.3				4	±	1
Y	55	±	1				33	±	8
Zr	180	±	4				183	±	9
Nb	101	±	2				74	±	4
Pb	38	±	2						
Th	21	±	2	23.7	±	0.2			

Figure Captions

Figure 1 Schematic diagram of the x-ray spectrometer employed.

Figure 2 Plot of the ratio of the two Compton scattered radiations measured (AgKB/AgKA) using stacked thin sections of quartz.

Figure 3 Relative response curve established for the excitation and detection of characteristic K-α spectral lines from a range of elements.

Figure 4 Flow chart of the steps undertaken for the determination of thirteen trace and three major elements in obsidian artifacts.

Figure 5 Photograph of four pieces of obsidian fractured from a single block of source obsidian from El Chayal.

Figure 6 X-ray spectrum acquired for the large piece of El Chayal obsidian.

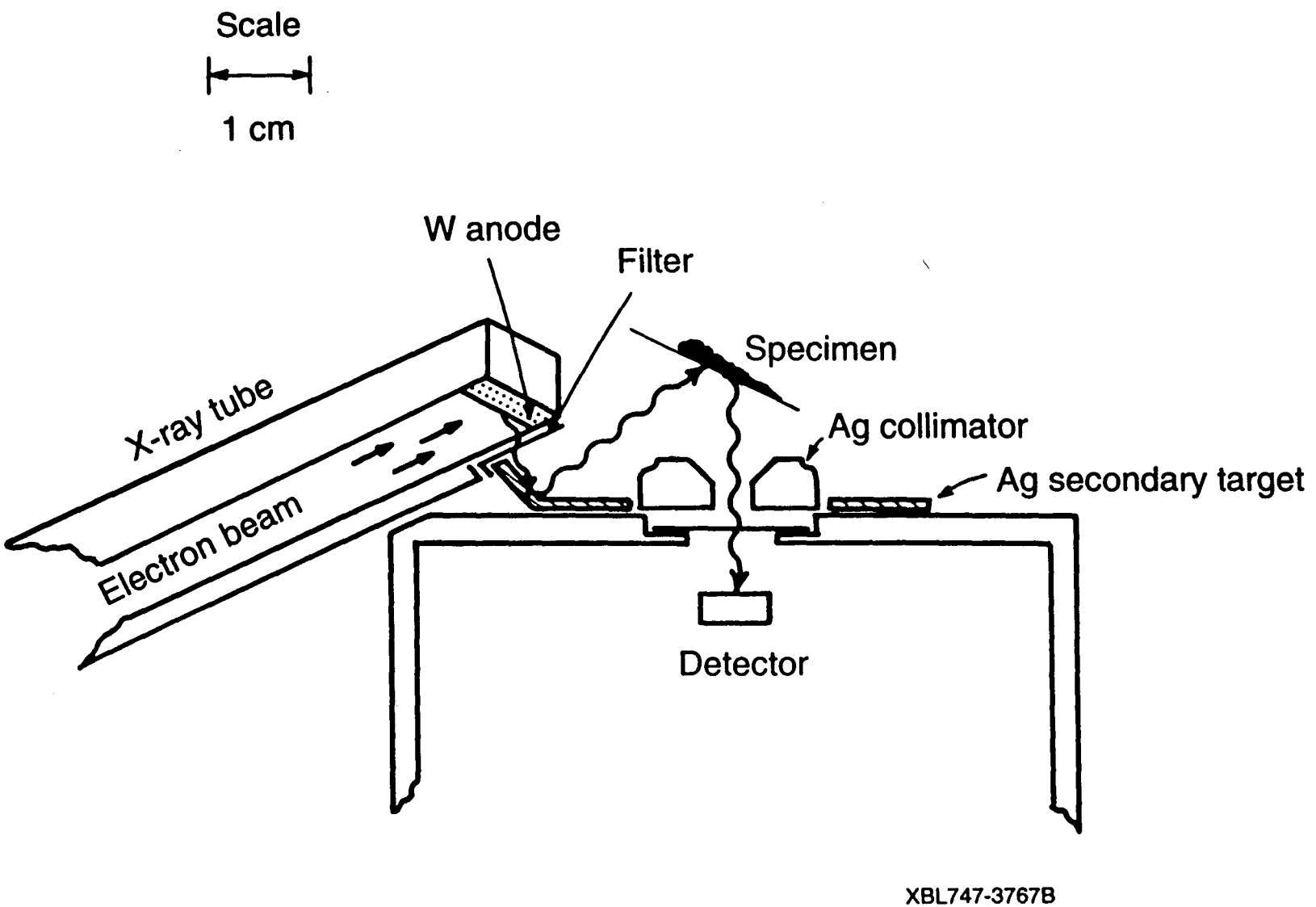
Scale
1 cm
W anode
Filter
Specimen
X-ray tube
Ag collimator
Ag secondary target
Electron beam
Detector
XBL747-3767B

FIGURE 1

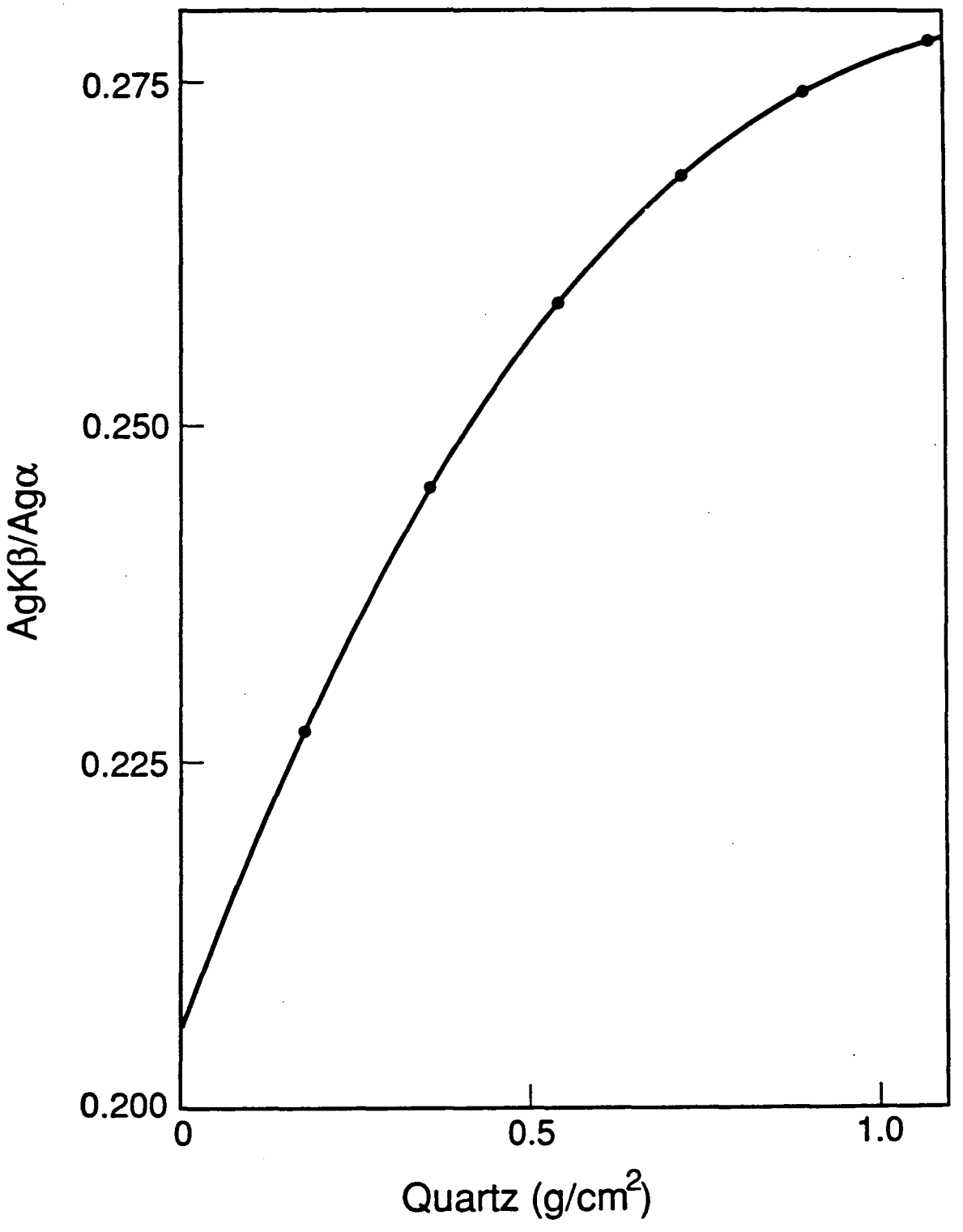

XBL 9010-5944

FIGURE 2

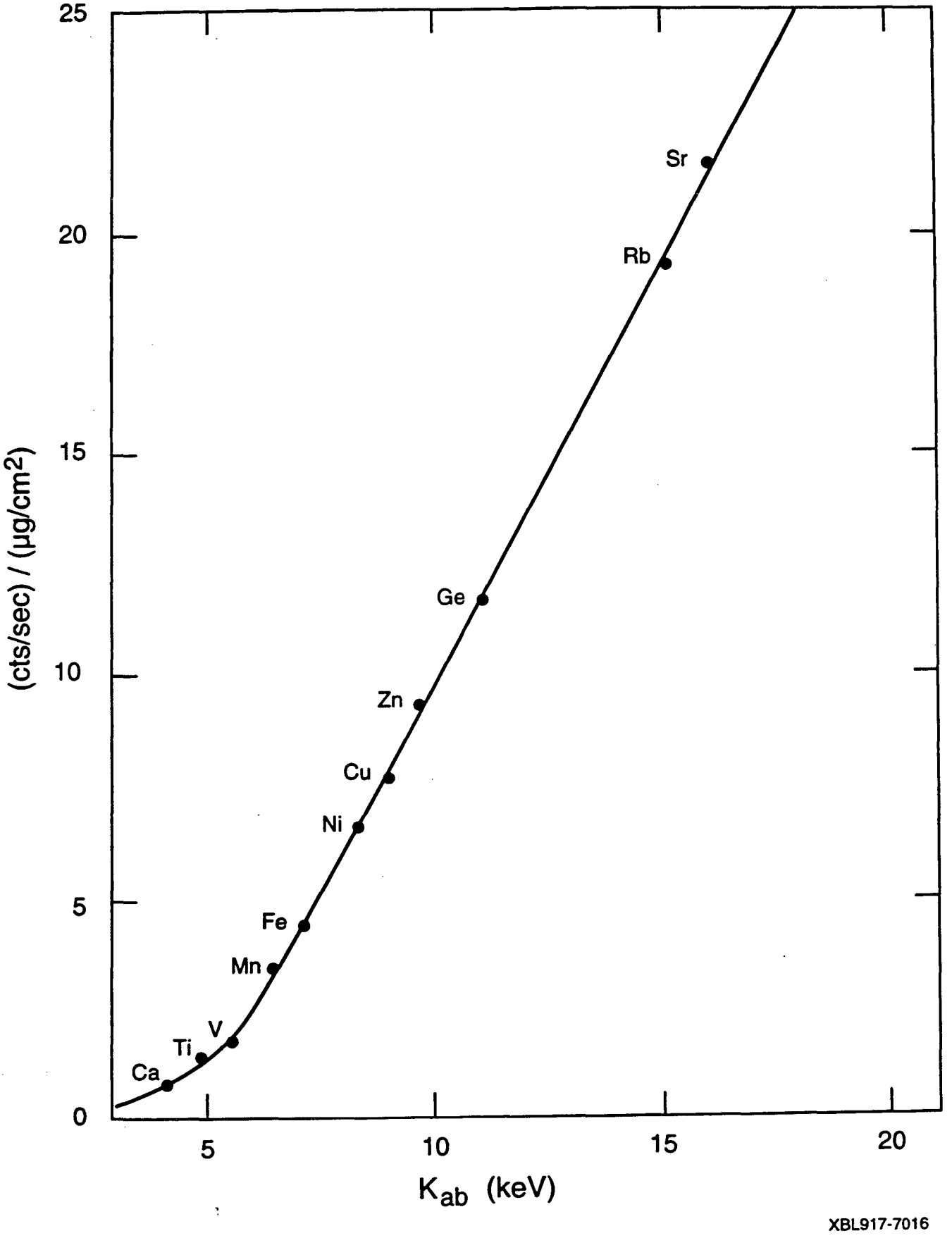
25
20
15
10
5
0
(cts/sec) / (μg/cm²)
5
10
15
20
K_ab (keV)
Sr
Rb
Ge
Zn
Cu
Ni
Fe
Mn
V
Ti
Ca
XBL917-7016

FIGURE 3

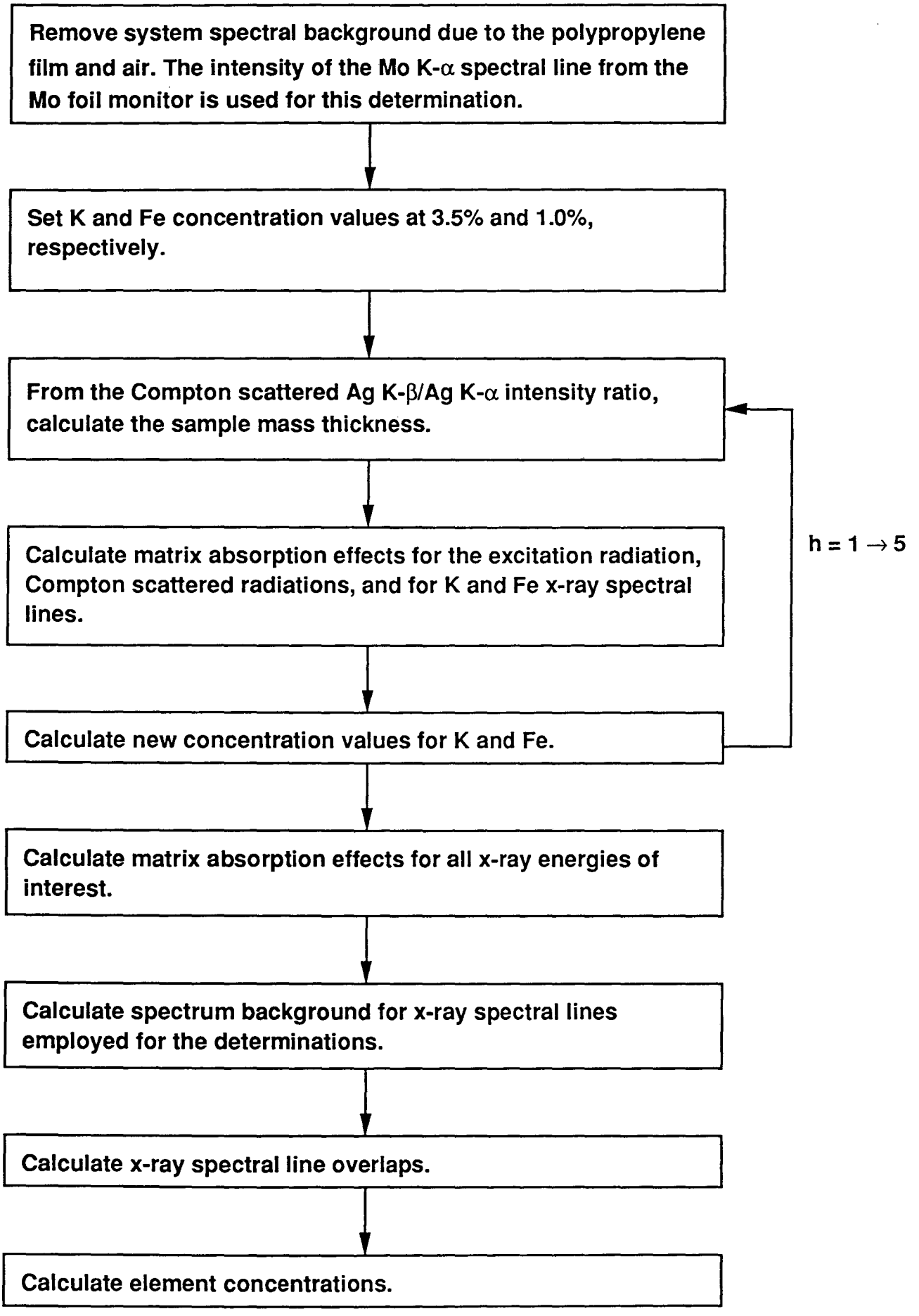
Remove system spectral background due to the polypropylene film and air. The intensity of the Mo K-α spectral line from the Mo foil monitor is used for this determination.
Set K and Fe concentration values at 3.5% and 1.0%, respectively.
From the Compton scattered Ag K-β/Ag K-α intensity ratio, calculate the sample mass thickness.
Calculate matrix absorption effects for the excitation radiation, Compton scattered radiations, and for K and Fe x-ray spectral lines.
Calculate new concentration values for K and Fe.
h = 1 → 5
Calculate matrix absorption effects for all x-ray energies of interest.
Calculate spectrum background for x-ray spectral lines employed for the determinations.
Calculate x-ray spectral line overlaps.
Calculate element concentrations.

FIGURE 4

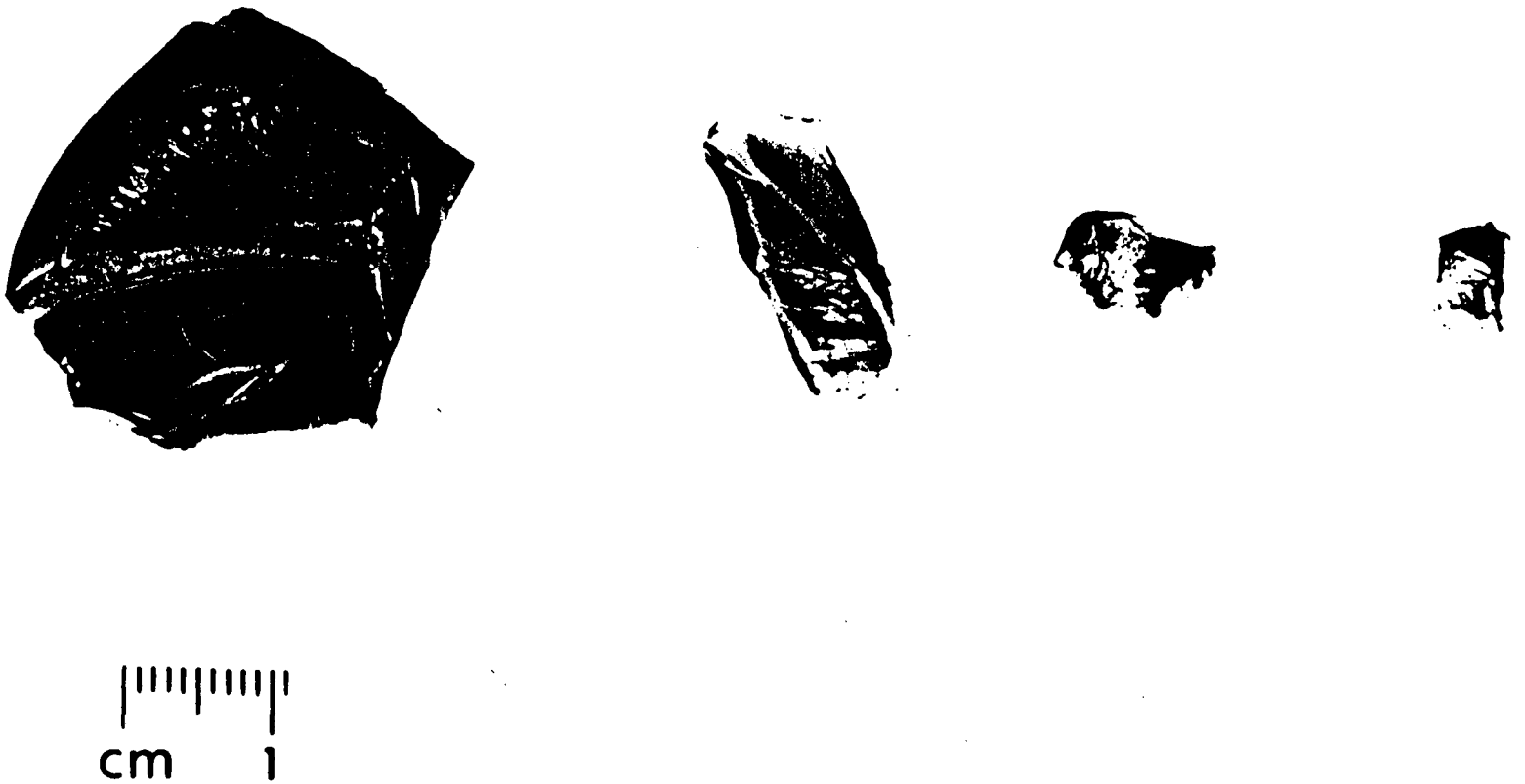

FIGURE 5

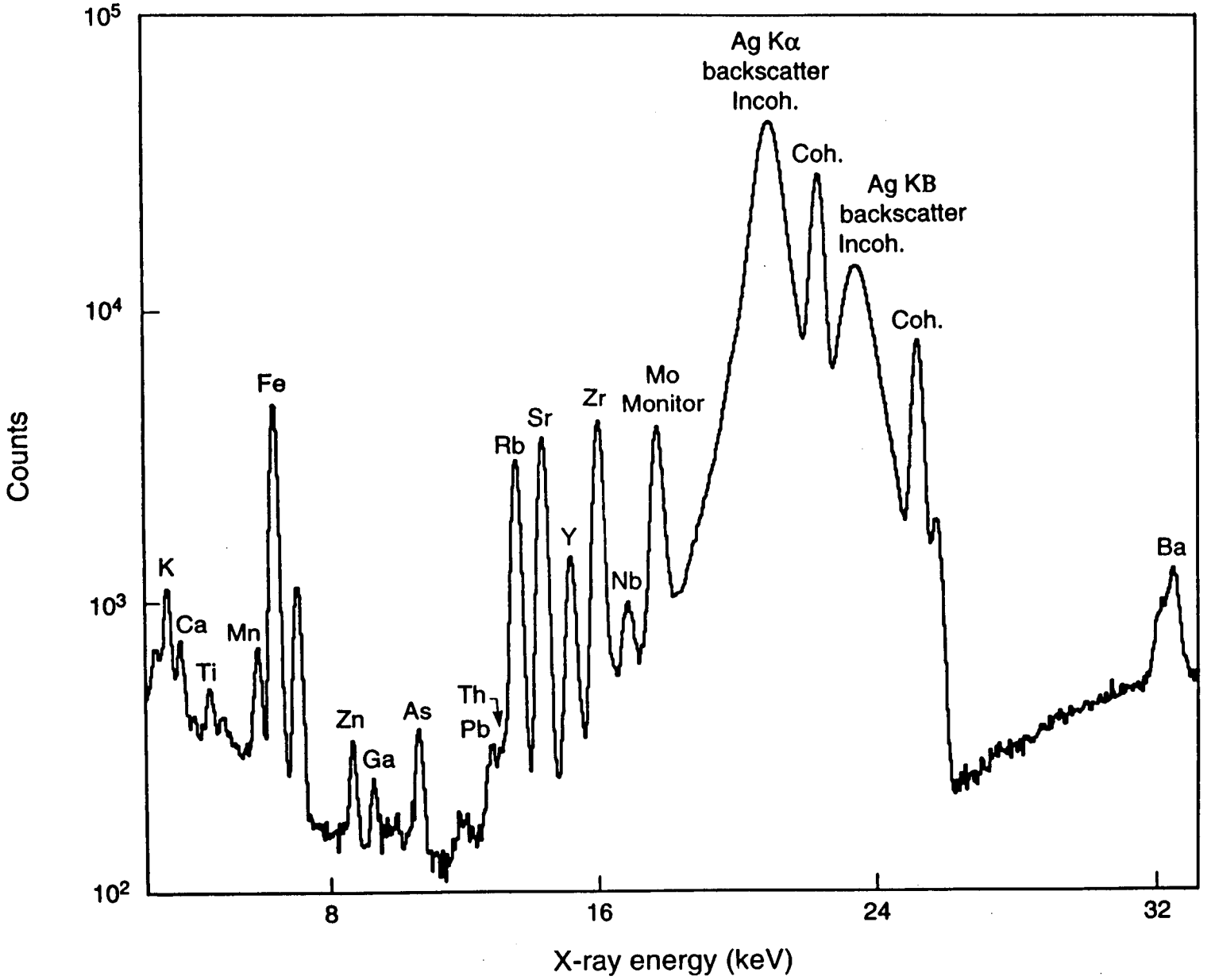

XBL 9111-6870

FIGURE 6

LAWRENCE BERKELEY LABORATORY
UNIVERSITY OF CALIFORNIA
TECHNICAL INFORMATION DEPARTMENT
BERKELEY, CALIFORNIA 94720